

Fig. 1. High-resolution FE-SEM image of chondritic IDP L2008E4. The scale bar equals 1 μm .

al and rectangular euhedral crystals varying from several hundred nanometers to several micrometers in size throughout the whole particle. In the case of a compact particle (L2009K18), which appears partly melted in the SEM, the interior consists of small crystals set into an amorphous matrix.

Morphological features and interior textures correlate well in these and other cases. It looks very promising that a database containing a wide variety of IDP surface features and correlated interior textures can serve as a tool for interpreting AFM images acquired during the ROSETTA mission.

References: [1] Whipple F. L. (1987) *Astron. Astrophys.*, 187, 852–858. [2] Schwehm G. (1995) *ESA-SP-1179*, 28–30. [3] Riedler W. et al. (1996) *COSPAR*, Elsevier, in press. [4] Romstedt J. et al. (1997) *Scanning*, 19(3), 142–143.

SILICA-BEARING OBJECTS IN BALI (CV3): A NOVEL TYPE OF INCLUSION IN CARBONACEOUS CHONDRITES. M. A. Nazarov¹, G. Kurat², and F. Brandstätter², ¹Vernadsky Institute of Geochemistry and Analytical Chemistry, Moscow, 117975, Russia, ²Naturhistorisches Museum, Postfach 417, A-1014 Vienna, Austria.

Introduction: Silica-bearing objects are common accessory constituents of ordinary and enstatite chondrites [e.g., 1]. Their origin is not clear and nebular and parent-body processes have been proposed for the formation of these objects [1–6]. Free silica is extremely rare in carbonaceous chondrites and has so far been found only in Murchison [7] and in a carbonaceous clast from the Erevan howardite [8]. Here we report on abundant silica-rich objects in a dark inclusion (DI) from the Bali (CV3) carbonaceous chondrite. This is a new type of silica-bearing object in chondritic matter. The origin of these objects could be related to nebular metasomatic alteration of CAIs.

Results: The Bali specimen I 2662 (Naturhistorisches Museum, Vienna) contained a dark inclusion of about 6 × 5 × 4 mm dimension highly enriched in magnetite as compared to the Bali host (in which pentlandite and pyrrhotite are the most abundant opaque phases). The matrix of the DI is porous and consists mainly of intergrowths of platy olivines rich in FeO (30 wt%), NiO (2%), and magnetite. This inclusion also contains about 1 vol% of silica-rich objects that resemble CAIs in their appearance (Fig. 1). The small objects are rounded and have dimensions of 10–20 μm . The larger objects are elongated and their sizes range from about 20 × 30 μm to 10 × 50 μm . The objects have a concentric structure with a core of mainly very fine-grained, dense silica. This silica has a variable chemical composition and is rich in minor elements (Al₂O₃: 0.2 wt%; FeO: 2.5; MgO: 0.6; NiO: 4.0; CaO: 0.3; and Na₂O: 0.1). In particular, the high contents of NiO (3.0–8.0 wt%) are remarkable. Some places are rich in Al₂O₃ (up to 2.5%) or P₂O₅ (up to 1.4%). Minor phases are wollastonite, andradite and Ca-rich pyroxene. A Ni-rich silicate (up

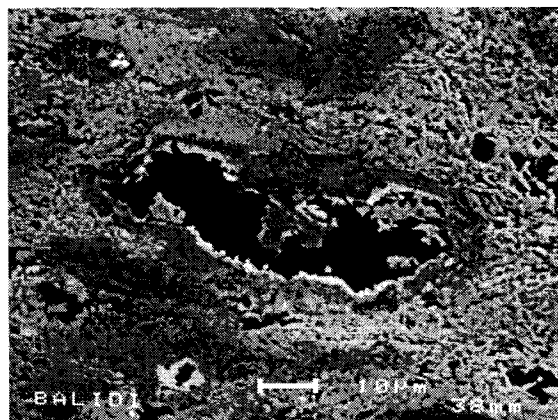


Fig. 1. SiO₂-rich object in a DI from Bali (CV3). Silica (dark), hedenbergite (light inner rim), diopside (dark outer rim) in olivine matrix.

to 30% NiO) was also found, but it is too small for identification. One object contains a small (3 μm) grain of larnite associated with wollastonite and andradite.

Beside silica-rich objects there are wollastonite-rich inclusions in the Bali DI that are up to 70 μm in size and have a rounded or irregular shape. They consist mainly of relatively coarse-grained wollastonite that contains rare minute grains of diopside, hedenbergite, and andradite. Some of the inclusions also contain free silica.

Silica-rich and wollastonite objects are always covered by two rims (each about 5 μm thick). The inner layer is made of hedenbergite, whereas the outer layer consists of salite or diopside. Sulfur and Ni are often present in the rims.

Discussion: The free silica is certainly of secondary origin and out of equilibrium with the chondritic, olivine-rich matrix. The shapes and the presence of Ca phases (including diopside) and rims suggest CAI precursors. The sequence of alteration events is not clear. The conditions must have been highly oxidizing (Fe, Mn, and Ni metasomatism of olivine and pyroxene, formation of andradite, hedenbergite, magnetite). Free silica is dense and had to be added to the inside of the objects. It is not clear why SiO₂ was deposited there. A possible hint is given by wollastonite, which possibly formed from CaCO₃ by reaction with SiO₂. Thus, it is possible that reactive Ca-rich phases of preexisting CAIs were carbonatized first and then silicified. Because there are no traces of Si mobility in the DI matrix, which consists mainly of olivine, these metasomatic reactions must have taken place before accretion.

Acknowledgments: This work was supported by the Austrian FWF and the Austrian Academy of Sciences.

References: [1] Brigham C. A. et al. (1986) *GCA*, 50, 1655–1666. [2] Krot A. and Wasson J. (1994) *Meteoritics*, 29, 707–718. [3] Olsen E. J. et al. (1981) *EPSL*, 56, 82–88. [4] Ruzicka A. et al. (1995) *Meteoritics*, 30, 57–70. [6] Bridges J. C. et al. (1995) *Meteoritics*, 30, 715–727. [7] Olsen E. J. (1983) in *Chondrules and Their Origins* (E. A. King, ed.), pp. 223–234, LPI, Houston. [8] Nazarov M. A. et al. (1995) *LPS XXVI*, 1031–1032.

MEASUREMENT OF GAS-PHASE SPECIES DURING LANGMUIR EVAPORATION OF FORSTERITE. R. H. Nichols Jr.^{1,2}, R. T. Grimley³, and G. J. Wasserburg¹, ¹Division of Geological and Planetary Sciences, Mail Stop 170-25, California Institute of Technology, Pasadena CA 91125, USA (isotopes@gps.caltech.edu), ²Present address: Department of Earth and Planetary Sciences Washington University, One Brookings Drive #1105, St. Louis MO 63130, USA (rhn@levee.wustl.edu), ³Department of Chemistry, Purdue University, West Lafayette IN 47907, USA (rgrimley@wcic.cioe.com).

Forsterite, the most abundant mineral in meteorites, forms at high temperatures often associated with nebular processes. It evaporates con-

gruently, and its equilibrium evaporation is rather well understood [e.g., 1]. For these reasons, in part, many recent studies have focused on the more difficult kinetics of the free (Langmuir or nonequilibrium) evaporation of this mineral [2–4]. Isotopic fractionations of Mg, Si, and O measured in residues of forsterite melts (m.p. ~1890°C) have been associated with the evaporation of specific vapor-phase species based on detailed isotopic and mass-balance analyses of the evaporative residues [2–4]. In particular, the isotopic fractionations of Si and O are attributed to kinetic or mass-dependent effects, which many workers have associated with the evaporation of SiO_2 [2–4]. In these studies, however, the identities of the dominant vapor-phase species have not been measured directly but have only been inferred, and these inferences are not in agreement with what one would expect from equilibrium evaporation where SiO is the dominant Si-bearing species [5]. In this work we have evaporated forsterite at high temperatures in both Knudsen (equilibrium) and Langmuir (non-equilibrium) configurations and have directly measured the atomic and molecular species present in the gas phase using quadrupole mass spectrometry with an electron-impact ionization source. The dominant Si-bearing species is SiO in both cases.

In the Knudsen configuration, for which preliminary results were previously reported [5], the forsterite sample (solid, Fo_{90}) was cycled from 1300°–1600°C in 30°–50°C steps. Dominant species detected include Mg, SiO , O, and O_2 . Measured SiO/SiO_2 ratios between 100–200 are similar to those observed during the equilibrium evaporation of solid SiO_2 [6] and to those expected from theory. Enthalpies and entropies of reaction computed from van't Hoff plots are in good agreement with those computed from equilibrium thermodynamics for the following evaporation reactions: (1) $\text{Mg}_2\text{SiO}_4(\text{s,l}) = 2\text{Mg}(\text{g}) + \text{SiO}(\text{g}) + 3\text{O}(\text{g})$; (2) $\text{Mg}_2\text{SiO}_4(\text{s,l}) = 2\text{Mg}(\text{g}) + \text{SiO}(\text{g}) + 1.5\text{O}_2(\text{g})$; (3) $\text{Mg}_2\text{SiO}_4(\text{s,l}) = 2\text{Mg}(\text{g}) + \text{SiO}_2(\text{g}) + 2\text{O}(\text{g})$; and (4) $\text{Mg}_2\text{SiO}_4(\text{s,l}) = 2\text{Mg}(\text{g}) + \text{SiO}_2(\text{g}) + \text{O}_2(\text{g})$.

In the Langmuir configuration, a sample of pure forsterite (Fo_{100}) was heated to temperatures below and above its melting point. Free-evaporation from the solid and liquid produces $\text{SiO}/\text{SiO}_2 \gg 1$ in the vapor phase, similar to values attained in the Knudsen case. Back-reactions or dissociation of SiO_2 within the experimental apparatus, both of which would tend to enhance the SiO/SiO_2 ratio, are considered to be negligible effects. The present study strongly suggests that Si and O isotopes are mass fractionated by the evaporation from liquid forsterite of SiO and not SiO_2 , contrary to inferences by other workers [2–4]. Relative abundances of detected species indicate that forsterite evaporates primarily via the reaction (1) above. The free evaporation rate is significantly lower than the equilibrium evaporation rate, as has previously been noted in the prior mass-loss studies [2–4]. This reduced rate suggests the presence of a kinetic barrier impeding evaporation, for which we calculate an activation energy of 410 ± 33 kJ/mol for Mg and SiO in reaction (1). The results of this study, coupled with the results of [2–4], may preclude simple Rayleigh distillation from an homogenized reservoir as a source for some of the gross isotopic effects observed in laboratory studies of forsterite and possibly in other meteoritic materials.

Acknowledgments: Supported by NASA grant NAGW3337 (GJW). Div. Cont. 8519 (999).

References: [1] Nagahara and Ozawa (1996) *GCA*, 60, 1445. [2] Davis et al. (1990) *Nature*, 347, 655. [3] Hashimoto (1990) *Nature*, 347, 53. [4] Wang (1995) Ph.D. thesis, Chicago, 151 pp. [5] Nichols et al. (1995) *LPS XXVI*, 1047. [6] Porter et al. (1955) *J. Chem. Phys.*, 23, 216.

STRONTIUM ISOTOPES IN SINGLE PRESOLAR SILICON CARBIDE GRAINS. G. K. Nicolussi^{1,2}, M. J. Pellin¹, R. S. Lewis², A. M. Davis², R. N. Clayton^{2,3,4}, and S. Amari⁵, ¹Materials Science and Chemistry Division, Argonne National Laboratory, Argonne IL 60439, USA, ²Enrico Fermi Institute, University of Chicago, Chicago IL 60637, USA, ³Department of Chemistry, University of Chicago, Chicago IL 60637, USA, ⁴Department of the Geophysical Sciences, University of Chicago, Chicago IL 60637, USA, ⁵McDonnell Center for the Space Sciences, Washington University, St. Louis MO 63130, USA.

Eleven individual SiC grains from the Murchison meteorite were analyzed for their Sr-isotopic compositions by laser ablation combined with

resonant ionization mass spectrometry. The majority of the analyzed grains have $^{87}\text{Sr}/^{86}\text{Sr}$ and $^{88}\text{Sr}/^{86}\text{Sr}$ ratios that are normal within the experimental uncertainties. However, large deficits were found for the p-isotope ^{84}Sr . The Sr-isotopic data found for these 11 grains are consistent with the s-process at low neutron densities in which the nucleosynthesis of Sr is affected by β decay of short-lived ^{85}Kr ($T_{1/2} \sim 10.8$ yr).

Introduction: Circumstellar dust grains found in a variety of primitive meteorites condensed from stellar outflows or from stellar explosion ejecta and provide important constraints on nucleosynthesis theory [1]. Most presolar SiC grains isolated from these meteorites have light element isotopic compositions consistent with formation around AGB stars [2]. In previous analyses we have measured isotopic abundances of Zr and Mo in presolar SiC [3,4]. The large and variable s-process enrichments in Zr and Mo seen in “mainstream” SiC are also entirely consistent with grain formation in the H-envelope of AGB stars. Strontium measurements on aggregates of Murchison SiC grains have shown large negative $\delta^{84}\text{Sr}/^{86}\text{Sr}$ values but very small variations in $\delta^{87}\text{Sr}/^{86}\text{Sr}$ and $\delta^{88}\text{Sr}/^{86}\text{Sr}$ [5].

Experimental: The Sr-isotopic composition was measured on the CHARISMA instrument using resonant ionization mass spectrometry to selectively ionize and detect the Sr isotopes [3,4,6]. The SiC grains used here are from the Murchison KJG fraction with a typical grain size of ~2–4 μm in diameter. Prior to isotopic analysis, the SiC grains were mapped with a scanning electron microscope.

Results and Discussion: Strontium has four stable isotopes. Strontium-84 is a p-process isotope that is shielded from the s- and r-processes. Strontium-86 is a pure s-process isotope, shielded from the r-process by ^{86}Kr . Strontium-87 is also an s-process isotope; however, it can be produced by decay of ^{87}Rb ($T_{1/2} \sim 48$ Ga). Strontium-88 is mainly an s-process isotope, but it has some r-process contributions in its terrestrial composition. In Fig. 1 the results for 11 individual SiC grains are shown in the form of three-isotope plots in which ^{86}Sr was used for normalization. Generally, very large deficits in the abundance of the p-isotope ^{84}Sr were found, which is consistent with s-process nucleosynthesis [7]. The solar-like $^{87}\text{Sr}/^{86}\text{Sr}$ reflects that their ratio depends only on the relative neutron capture cross sections. Synthesis of ^{86}Sr and ^{87}Sr requires that the s-process path runs from ^{84}Kr to ^{85}Rb to ^{86}Sr via the unstable nuclei ^{85}Kr and ^{86}Rb . Because of the predominant β decay at the ^{85}Kr branch an upper limit for the neutron density at the s-process site can be inferred [8]. Decay of ^{87}Rb contributes very little to the ^{87}Sr abundance in the SiC grains. Two grains have significantly enhanced $^{88}\text{Sr}/^{86}\text{Sr}$ ratios and very low $^{84}\text{Sr}/^{86}\text{Sr}$ ratios. This indicates neutron capture on ^{85}Kr that bypasses the synthesis of ^{86}Sr and ^{87}Sr but would produce ^{88}Sr . Generally, the $^{88}\text{Sr}/^{86}\text{Sr}$ ratios show a much larger spread compared to analyses on SiC aggregates [5].

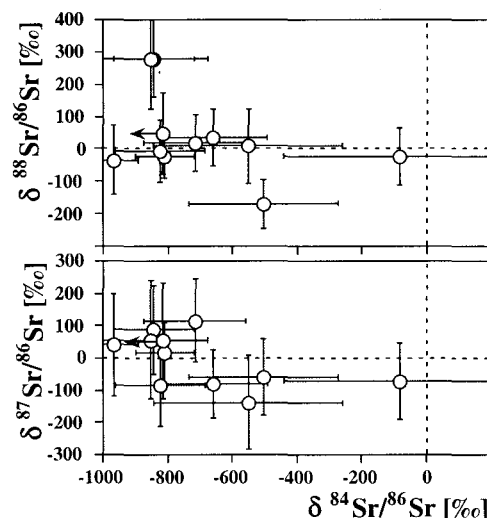


Fig. 1. Three-isotope plots of Sr from 11 individual SiC grains (error bars $\pm 2\sigma$).